Optimal Configuration and Placement of PV Systems in Building Roofs with Cost Analysis

Optimal Configuration and Placement of PV Systems in Building Roofs with Cost Analysis

Matteo Orlando, Lorenzo Bottaccioli, Edoardo Patti, Enrico Macii, Sara Vinco and Massimo Poncino
Politecnico di Torino, Turin, Italy. Email: name.surname@polito.it

***Abstract*—Following the Smart Grid view, current energy generation systems based on fossil fuels will be replaced with renewable energy sources. Photovoltaic (PV) is currently considered the most promising technology, due to decreasing costs of the devices and to the limited invasiveness in existing infrastructures, that make PV installations quite common urban buildings' roofs. To maximise both power production and Return Of Investment (ROI) of PV installations, new techniques and methodologies should be applied to limit sources of inefficiencies, like shading and power losses due to an incorrect installation. In this paper, we propose a novel solution for an optimal configuration and placement of PV systems in buildings' roofs. Given a number of alternative configurations and a roof of interest, it combines detailed geographic and irradiance information to determine the optimal PV installation, by maximizing both power production and ROI. Our simulation results on two real-world roofs demonstrate an improvement on power generation up to 23% w.r.t. standard compact installations. These results also highlight that a cost analysis, often ignored by standard installation strategies, is nonetheless necessary to guarantee optimal results in terms of PV production and revenue.**

***Index Terms*—Photovoltaic installation, Reneawable Energy Simulation, PV design, PV optimization, GIS-based design.**

I. Introduction

One of the main challenges in nowadays societies consists of reducing energy consumption and CO_2 emissions to contrast global warming [1]. This is fostering a replacement of energy generation based on fossil fuels with renewable energy sources. Photovoltaic (PV) is probably the most popular and widespread technology, thanks to its limited costs and to an easy installation in urban contexts (e.g., on roofs of existing buildings).

Placement of PV systems in buildings' roofs should be carefully designed to maximise both the power production and, consequently, the Return Of Investment (ROI). To this extent, it is necessary to avoid any source of inefficiency: PV modules must be installed in areas with the best conditions in terms of solar irradiance, so to limit the impact of shading and the consequent power losses. At the same time, it is crucial to take into account the economic dimension, to guarantee that the initial investment is compensated by revenues over time, and and adequate ROI. This can not be achieved by traditional PV installation techniques, that are based on rule-of-thumb criteria.

This work proposes a framework to achieve an optimal PV installation, both in terms of power production and ROI. The key enabling technology is a GIS-based approach to generate irradiance and temperature evolution over the roof over one year. Such fine-grained and detailed information allows to determine which areas of the roof are more promising, as less affected by shading caused by encumbrances (e.g., nearby buildings, trees, dormers). To minimize power losses caused by partial shading and by an inefficient connection of the PV modules, we additionally analyse the correlation between the irradiance evolution over time of different areas of the roof, to guarantee that bottleneck effects are if not completely avoided at least limited.

This leads to the definition of an effective exploration over a number of possible configurations: for each configuration, we determine the optimal placement and connection of PV modules, trying to maximize irradiance and to minimize sources of inefficiencies. The irradiance and temperature data are then used to estimate the yearly power production of each installation, and to derive the corresponding ROI and the Payback Time (PT) of the investment. The result is the identification of the optimal configuration, in terms of both power production and revenues.

To prove the effectiveness of the proposed framework, we applied the analysis to two roofs of industrial buildings. Results show an improvement on power generation from 11% up to 23% w.r.t. standard installations. Moreover the outcome highlights that a cost analysis, typically ignored by standard installation strategies, is crucial to determine the optimal installation, as more PV modules do not always guarantee the highest ROI.

The rest of the paper is organized as follows. Section II briefly introduces the technology behind the PV power generation. Section III reviews relevant literature solutions on this topic. Section IV presents the proposed methodology. Section V discusses the experimental results. Finally, Section VI provides the concluding remarks.

II. Photovoltaic power generation

A. PV hierarchy

The basic element of a PV generator is the *cell*, whose behaviour can be described by an ideal current source, proportional to solar irradiance, and by a diode connected in anti-parallel. A cell is described by a voltage-current (I-V) characteristic curve (right of Figure 1, black lines), which, at a given cell temperature, changes as a function of the irradiance G: when G increases, the open-circuit voltage V_{oc} increases logarithmically and the short-circuit current I_{sc} increases proportionally. With fixed irradiance G, a temperature increase yields a slight increase of I_{sc} and decrease of

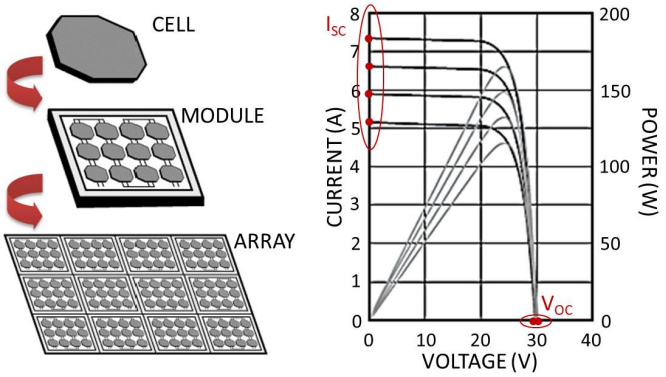

Fig. 1. PV hierarchy (left) and voltage-current (I-V) and voltage-power (P-V) characteristic curves of the Mitsubishi's PV-MF165EB3 PV module [2].

V_{oc}. The maximum of the corresponding voltage-power (P-V) curves (grey lines) corresponds to the optimal conditions for extracting power, given the current irradiance.

PV installations are organized hierarchically (left of Figure 1): cells are connected together into a PV *module*; PV modules can be further interconnected to form a *PV array* to achieve the desired voltage and current levels. The typical connection is organized as a number of parallel strings, each composed of the same number of PV modules connected in series.

B. Impact of uneven irradiance distribution

As anticipated in Section II-A, irradiance has a heavy impact on the power production of a PV module. PV installations are typically designed by assuming that the surface of interest is subject to even irradiance. This is however not accurate, as shadows projected by obstacles such as chimneys, surrounding buildings, trees, etc determine a heterogeneous distribution of irradiance, with the effect that each PV module will operate at different irradiance conditions. Shading is critical for PV installations, as the least irradiated PV module acts as a bottleneck on the power production of the overall installation: the higher the variance of irradiance, the higher the power loss. When PV modules are connected in series, the least irradiated module will provide the smallest current, thus restricting the available current of the string; when series strings are then connected in parallel, the string with lowest voltage will determine the voltage of all strings. This leads to a potentially high power dissipation, resulting in local overheating, accelerated ageing and permanent cell damage [3].

III. Related Works

Geographic Information Systems (GIS) are recognised as a key technology in modelling the evolution of solar irradiance and in simulating PV production [4]. GIS can also be used to plan installation of PV systems in urban environments [5]. For these purposes, such GIS-based solutions take advantages of *Digital Surface Model* (DSM) or 3D city models given by LiDAR data. DSM is a geo-referenced raster image representing the terrain's surface with all objects on it and elevation.

Efficient PV design and installation has been deeply investigated in the literature. In this scenario, solutions like [6]–[11] exploit both geographic data and evolution of shadows to estimate PV power production. However, they abstract the modelling of PV power production both in terms of model accuracy and placement topology of PV modules. In addition, these literature solutions do not integrate sub-hourly meteorological data needed to better estimate PV power production in real-sky conditions. PVGIS [8] and PVWatts [7] are the only exceptions performing hourly and sub-hourly simulations, respectively. However, they use a low-resolution DSM (i.e. $> 1m$) that is not suitable to identify encumbrances in roofs like chimneys and dormers. To achieve that, a DSM resolution smaller than $1m$ is needed. Moreover to perform realistic and accurate simulations, real meteorological data collected by weather stations [5] have to be used to compute the incident solar radiation on roofs in real-sky conditions. Finally, none of presented solutions provide guidelines for a smart, GIS-driven floorplanning of PV modules.

Other approaches focus on the optimal sizing of the PV installation [12]–[15], on the identification of optimal management algorithms [16], [17], or on optimal roof configuration (e.g., tilt angle) [18], by abstracting on the other aspects of PV designs. Vice versa, the works in [6], [19]–[21] focus on the identification of suitable areas at large (i.e., entire roofs or geographical areas), with no detailed information about the actual placement of PV modules and with very abstract models of PV power production. The work in [22] proposes an algorithm to exploit environmental traces to determine an optimal placement of PV modules. However, the traces are used only to determine heatmaps of the most promising locations on the roof, and it considers the configuration of the PV installation as a user-defined input, with no exploration of potential alternatives based on a cost analysis.

With respect to the literature, the approach proposed in this paper explores a number of alternative configurations and identifies the optimal one both in terms of power production (through a placement of PV modules that is aware of fine grain environmental traces) and of economic investment (highest ROI and lowest PT). Additionally, this work extends [22] with an analysis of the correlation of irradiance over time of different areas of the roof, to further minimize bottleneck effects.

IV. Methodology

The goal of the paper is to *determine an optimal configuration for a PV array through a design space exploration of a number of possible alternatives*. The first step generates traces of irradiance G and temperature T over time for the roof of interest, with a fine grain time and spatial granularity (A). Then, we determine a number of configurations of interest from user-defined input (B). For each configuration under analysis, we estimate an optimal placement of PV modules on the roof (C), estimate the corresponding yearly power production (D) and evaluate the foreseen payback time of the installation (E). This will allow to easily identify an

optimal configuration for the roof of interest (F), aware both of environmental quantities and of cost variables.

A. Irradiance and temperature traces for the roof of interest

The proposed PV floorplanning algorithm takes advantage of fine-grain resolution maps of irradiance and temperature, generated by exploiting the software infrastructure built in [23]. Given a high-resolution DSM of the roof of interest, the software identifies encumbrances (e.g. chimneys and dormers) and estimates the evolution of possible shadows. With such information, it is possible to perform the identification of the suitable area of the roof that can be used for the placement of PV panels, that is then aligned to a *virtual grid* with fine grain space granulatity (20cm), used by the PV placement algorithm. The evolution of irradiance over time is obtained by combining weather data, retrieved from personal or third-party weather stations [24], with the shadow model. Weather temperature and incident irradiance are then used to determine the distribution of temperature on roof over time, as an effect of convectivity and radiative loss [23]. The result are a set of measures of irradiance $G(i,j,t)$ and temperature $T(i,j,t)$, each associated with a grid cell in position (i,j) at a given time step t, with 15 minutes granularity.

B. Available configurations

Each configuration considered in the exploration is identified by the number of PV modules N_i to be placed on the roof. All configurations have the same connection topology: they are organized as strings of s PV modules in series, with s given in input by the user. Thus, different configurations vary in terms of number of strings connected in parallel $p_i = \frac{N_i}{s}$. The number of modules is limited by a maximum N_{MAX}:

- *user-defined*: the user gives in input the maximum number N_{MAX} of PV modules that can be explored;
- *cost-defined*: the user specifies a maximum budget B that can be invested and the cost $unit\_cost$ of a single PV module of interest; thus $N_{MAX} = \frac{B}{unit\_cost}$.

If N_{MAX} is too large for the suitable area, N_{MAX} is set to the maximum number of PV modules that can be hosted.

C. Optimal PV placement

Given an input configuration $N_i = s \times p_i$ of PV modules to be installed, the goal of the placement algorithm is to exploit the environmental traces $G(i,j,t)$, $T(i,j,t)$ to identify an optimal placement and connection of the PV modules on the roof. Given that an exhaustive exploration of the possible solutions is not feasible for roofs of a reasonable size [22], the algorithm builds an approximation of the optimal solution based on a suitability metric.

a) Suitability metric: The most promising positions for a PV module are those guaranteeing a higher irradiance over time. The suitability metric $S(i,j)$ of a cell position (i,j) should thus give an aggregate measure of the potential PV production that can be achieved when placing the top left corner of a PV module in (i,j). The suitability metric $S(i,j)$ is the *75-th percentile* of irradiance, that represents the value below which 75% of the samples of $G(i,j,t)$ fall for grid position (i,j): larger values of the percentile identify distributions that are more skewed towards the upper range of the values. The suitability metric $S(i,j)$ is then applied a corrective factor, modeling the impact of temperature[1].

b) Similarity metric: Connecting PV modules with similar irradiance over time is especially important when connecting PV modules in series[2]: e.g., the placement algorithm must avoid the series connection of PV modules that have similar suitability metric but that are on the opposite sides of an obstacle, with the result that when the one is in full sun the other is shaded, and vice versa. A measure of similarity between two grid cells (i,j), (i',j') is given by the correlation of their irradiance traces over time, i.e., a measure of how linearly dependent the traces of $G(i,j,t)$ and $G(i',j',t)$ are over time. This is estimated by calculating the Pearson correlation coefficient of the irradiance traces: a high correlation coefficient ensures that two PV modules placed in (i,j) and (i',j') would behave similarly.

c) PV placement algorithm: The resulting PV placement algorithm is given in Figure 2. First (line 1) the suitability matrix S is computed as described above for all grid cells. Grid cells are then sorted in decreasing order of S in vector V: the first cells are the most promising ones (i.e., higher 75^{th} percentile of irradiance). We then iterate the choice of the placement of the Ni PV modules to be placed in series-first order, i.e., modules belonging to a series string are enumerated before moving to another string. When choosing the position of the first PV module of a series string (lines 5-8), we pick the grid cell with highest suitability metric (i.e., $V[1]$). When choosing the placement of the subsequent $s-1$ PV modules of the string (lines 10-18), we must take into account the correlation of their irradiance traces w.r.t. the first PV module of the series ($first$). To this extent, we introduce a threshold th: given the grid cell with highest suitability matrix $V[l]$, it is added to the series only if its correlation w.r.t. $first$ is higher than th. Else, the algorithm moves to evaluating the next position. Note that any time the placement of a PV module is chosen, all grid cells covered by the module become unusable and are thus removed from vector V. The loop terminates when the Ni PV modules have been placed.

D. Estimation of yearly power production

Given the placement of PV modules, it is necessary to derive the corresponding yearly power production.

1) PV module model: The power production of each PV module is determined with the model proposed in [22], [27], that exploits information available in public datasheet of the PV module to build a simple linear model. Power dependency on G and T is determined from the thermal and irradiance coefficients and the I-V graphs in the datasheets, respectively. The result are linear equations of current $I(i,j,t,G,T)$ and

[1]Temperature is considered only as a corrective factor as its impact on power production is limited w.r.t. irradiance (less than 0.5%/°C) [25].

[2]The bottleneck effect is heavier in case of series connection, as module voltage has a weaker dependence on irradiance than current [26].

```
Input:    grid: roof representation as a grid of cells
          Ni, s, p: number of PV modules (Ni) and topology (s x p)
          G(i; j; t) ,T(i; j; t): environmental traces
          th: correlation threshold
Output:   plcmt: list of positions of the top left corner of PV modules
1.  Calculate the suitability matrix S(i, j) of each grid cell (i, j) from G and T
2.  Sort grid cells in non decreasing order of suitability in vector V
3.  k = 1
4.  while k < Ni {
5.      if (k%s == 1) {
6.          plcmt[k] = V[1]
7.          remove V[1] and all grid cells covered by placement in V[1]
8.          first = k
9.      } else{
10.         assigned = 0
11.         while assigned == 0{
12.             l = 1
13.             if correlation(plcmt[first], V[l]) > th{
14.                 plcmt[k] = V[l]
15.                 assigned = 1
16.                 k = k + 1
17.                 remove V[l] and all grid cells covered by placement in V[l]
18.             } l = l + 1
19.         } k = k + 1
20. }   }
```

Fig. 2. Main steps of the proposed PV placement algorithm.

voltage $V(i, j, t, G, T)$, that linearly depend on the value of the environmental traces $G(i, j, t)$ and $T(i, j, t)$ in the given PV module position (i, j) at current time t. The linear models ensure fast construction and simulation time, thus reaching a good accuracy/speed trade off, crucial in a design space exploration, and allowing the evaluation of the yearly PV production of a high number of alternative configurations.

2) Topology application: Given the individual production of PV modules, the impact of their $s \times p$ series and parallel connection is as follows. We first consider the *series connection* of PV modules composing a string, where the PV module with the lowest current (i.e., irradiance) limits the current of the other PV modules, while string voltage is the sum of single PV module voltages. Then, we take into account the *parallel connection* of strings: the PV string with the lowest voltage constraints the voltage also of the other strings, while the current is the sum of currents generated by the single strings.

3) Yearly power production: Yearly power production P_{yearly} of the PV installation is estimated by applying the aforementioned formula to the traces of G and T over time. By accumulating power over all time samples gives thus an estimation of the yearly power production of the installation:

$$P_{yearly} = \sum_{t=1...T} V_{array}(t) \cdot I_{array}(t)$$

where T is the length of the environmental traces (i.e., 35,040, the number of 15-minutes samples in a year).

E. Cost analysis

In this work we use two metrics of the "goodness" of a configuration. The Return Of Investment (ROI) is a measure of efficiency of an investment:

$$ROI = \frac{yearly\ revenue - cost\ of\ installation}{cost\ of\ installation}$$

and it allows to compare the different configurations according to the gains provided in one year of operation. Payback Time (PT) is an indication of the amount of time that is needed to payback the initial investment:

$$PT = \frac{cost\ of\ installation}{yearly\ revenue}$$

In both formulas, the cost of installation is given by the unit cost of a PV module multiplied by the number of PV modules in the current configuration. The yearly revenue takes into account the amount of money earned by selling the generated power to the grid (calculated by multiplying the yearly kWh production of a configuration P_{yearly} per the price of energy E_p), minus the cost of maintenance M_c, originated by the periodic cleaning, monitoring and repairing of PV modules (e.g., panel damage, fractures, and frame corrosion) [28]. E_p and M_c are provided in input by the user.

F. Identification of optimal configuration

Given the yearly power production, the ROI and the PT of each configuration identified in Section IV-B, the optimal configuration is selected as the one that maximizes the ROI, while minimizing the PT. Notice that the solution with the highest number of PV modules may not be the optimal one, due to an increase not only of power production but also of the initial investment and of maintenance costs.

V. Results

A. Simulation setup

We applied the proposed algorithm on two lean-to roofs, reported in Figure 3 (black areas represent to the presence of encumbrances that do not allow PV module installation, e.g., pipes). Using the strategy in Section IV-A, we first generated the values of irradiance and temperature over one year. Figure 3 shows the 75^{th} percentile of irradiance over the roof, where the clearer cells are the more irradiated (i.e., highest suitability metric). The heterogeneity in color distribution highlights the high variance of irradiance distribution, despite of the relatively small size of roofs (roof 1 is 49m$\times$12m, roof 2 is 42.8m$\times$12m). In our setup, we consider a PV-MF165EB3 module by Mitsubishi [2], and the configurations of interest are generated by considering strings of $s = 8$ PV modules and $N_{MAX} = 72$, defined as user configuration.

B. Analysis of the proposed PV placement

To focus of the placement algorithm proposed in Section IV-C, we focus the analysis on two configurations per roof, i.e., with $N_i = 32$ and $N_i = 72$. Figure 4 compare three placements per each roof: a traditional "compact" placement (a,d), the placement generated by [22] (b,e), that only observes the distribution of irradiance on the roof, and the placement generated by the proposed algorithm (c,f). Table I reports the yearly power generation of each configuration, plus the

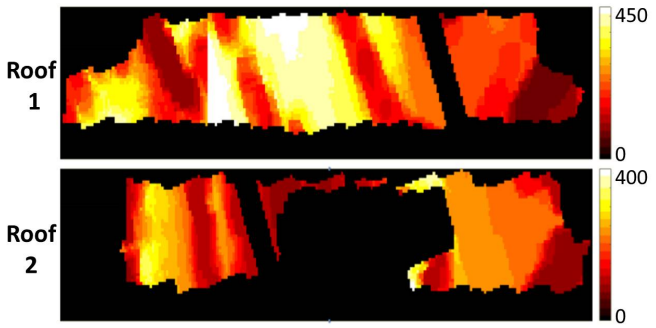

Fig. 3. 75^{th}-percentile of G over the roofs (the clearer the more irradiated).

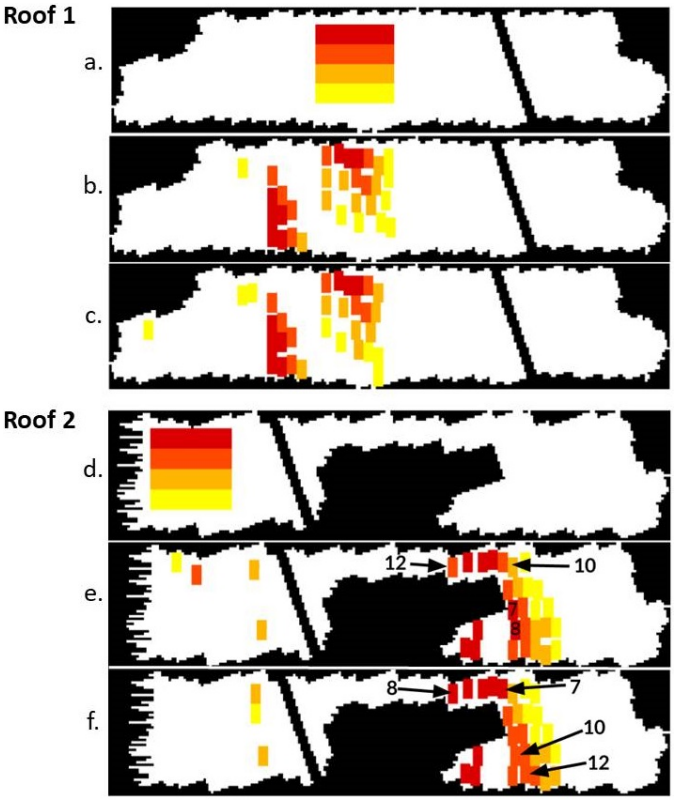

Fig. 4. Possible configuration for N=32 for roof 1 ($a-c$) and roof 2 ($d-f$): traditional "compact" placement (a,d), placement generated by [22] (b,e), proposed algorithm (c,f). Rectangles are PV modules, rectangles of the same color are PV modules connected in series.

TABLE I
YEARLY POWER PRODUCTION OF [22] AND OF THE PROPOSED ALGORITHM WITH RESPECT TO THE TRADITIONAL PLACEMENT

Roof	N	Traditional	[22]		Proposed	
		(kW)	(kW)	(%)	(kW)	(%)
Roof 1	32	6.21	6.94	11.70	7.01	12.80
	72	12.19	14.27	17.10	14.66	20.20
Roof 2	32	5.04	5.28	4.80	5.60	11.10
	72	9.37	11.25	20.00	11.57	23.00

improvement of [22] and of the algorithm proposed in this work (with threshold set to 0.9, i.e., correlation 90%) w.r.t. the traditional placement.

From Figure 4 it is clear that the *traditional placement*, that is extremely compact, is very different from the ones built by [22] and by the algorithm proposed in this work, that are rather scattered. By comparing the placements with the distribution of the 75^{th} percentile of irradiance (Figure 3) it is easy to notice that both [22] and the algorithm proposed in Section IV-C exploit the most irradiated areas, thus reaching a maximum improvement w.r.t. the traditional placement of 20% for [22] and of 23% for the proposed algorithm. This proves the importance of observing the evolution of environmental quantities on the roof of interest.

The differences between [22] and the algorithm proposed in this work are instead more subtle, and are mostly due to the fact that [22] ignores the correlation of irradiance evolution over time before actually placing the PV modules. The result is always an improvement of the proposed algorithm over [22], from a minimum of 1% to a maximum of 6%.

By looking at PV module placement for *roof 1* (Figure 4.a-c), we observe that the main variation is related to the placement of PV modules belonging to the last series (yellow). Our algorithm considers as more promising positions with a potentially lower suitable metric, but that are more highly correlated to the evolution of irradiance of the first module of the series. Also the other series differ between the two approaches, but in terms of connection of the PV modules, instead of placement. This is also explained by the fact that our algorithm gives priority to the correlation of irradiance evolution over time, rather than to the 75^{th} percentile per se, when connecting PV modules in series. This allows to minimize the bottleneck effect. For this roof, the larger the number of PV modules, the higher the benefit w.r.t. [22] ($+1.01\%$ for $N = 32$, $+2.73\%$ for $N = 64$): the benefit is higher when the placement has to adopt not only highly irradiated areas but also more shaded positions.

For *roof 2* (Figure 4.d-f), we notice not only that a few panels are in different positions, but also that the the most interesting changes regards how the PV modules are connected together: PV modules number 7 and 8 in our placement (and thus belong to series 1) are moved to series 2 in the placement proposed in [22] (position 10 and 12), and are replaced by PV modules originally connected to series 2. This different connection of the PV modules allows to reach a higher advantage over [22] also in the configuration with less PV modules ($+6.06\%$ for $N = 32$). This happens because our algorithm is particularly efficient when dealing with roofs that are highly subject to shadows, like the presence of pipes and dormers (the large black area in the middle). Such encumbrances increase the impact of considering not only the typical behavior of a grid cell (i.e., the 75^{th} percentile) but also the evolution of irradiance (i.e., of shadows) over time.

Overall, it is important to note that the proposed placement algorithm, that takes into account also shadow evolution over time, improves power production not only w.r.t. traditional placements, but also w.r.t. the current state of the art [22], with an improvement in the order of kW per year even in small installations.

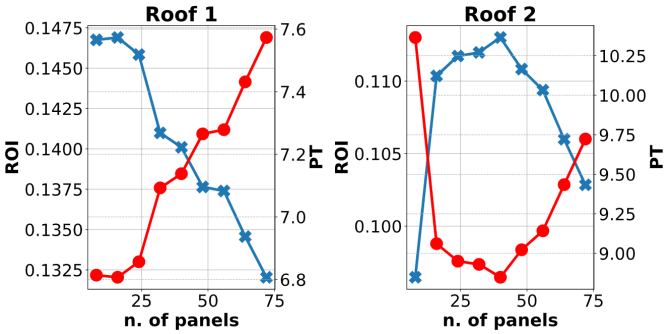

Fig. 5. Values of ROI (cross) and PT (circle) for roof 1 and 2 over the considered configurations (i.e., with varying N).

C. Cost analysis evaluation

The cost analysis was made by considering these parameters: $p_c = 250$, $E_p = 0.22\$/kWh$, $M_c = 15\$/kW/year$. By applying the methodology described in the previous section, we obtained the plots shown in Figure 5, which shows the ROI (crosses) and the PT (circles) for the two roofs when varying N (i.e., over the considered configurations). Notice that the evolution of PT is approximately the inverse of ROI (as evident from the equations).

The ROI behaviour for the first roof shows that the optimal configuration that maximizes the ROI (and minimizes PT) is not the one with the highest number of PV modules but rather the configuration with only 16 PV modules: adding more panels thus does not directly mean having better results in terms of investment, as the algorithm will continue to add panels in areas with decreasing irradiance: therefore the revenue does not grow linearly with N, as the increased power production does not compensate for higher investment and mainenance costs. A similar situation occurs for the second roof, that shows a parabolic trend: the addition of new panels can increase the ROI (i.e., decrease PT) up until the point when the ROI starts to decrease (i.e., PT starts increasing), with a maximum at $N = 40$.

VI. Conclusion

This work proposes an algorithm to find an optimal configuration for a PV installation, by observing both the cost dimension (e.g., in terms of number of PV modules and return of investment) and the power dimension (i.e., position and connection of PV modules). This allows to improve power production by up to 23% w.r.t. traditional placements and 6% w.r.t. the current state of the art [22]. Additionally, the exploration allows to derive non-intuitive optimization solutions, based on panel cost, energy price and maintenance cost, that ensure a cost-effective design of the installation and to avoid any loss of money due to a wrong sizing of the number of necessary PV modules. This shows how different scenarios require different investment strategies in order to maximize the profit of the PV investement.

References

[1] United Nations, FCCC, "Adoption of the Paris Agreement. Proposal by the President," 2015, Available: http://unfccc.int/resource/docs/2015/cop21/eng/l09r01.pdf.

[2] *PV-MF165EB3 Datasheet*, 2004, www.mitsubishielectricsolar.com.

[3] E. S. Kumar and B. Sarkar, "Improved modeling of failure rate of photovoltaic modules due to operational environment," in *Proc. of ICCPCT*, 2013, pp. 388–393.

[4] S. Freitas, C. Catita, P. Redweik, and M. Brito, "Modelling solar potential in the urban environment: State-of-the-art review," *Renew. Sustainable Energy Rev.*, vol. 41, pp. 915–931, 2015.

[5] B. Resch, G. Sagl, T. Törnros, A. Bachmaier, J.-B. Eggers, S. Herkel, S. Narmsara, and H. Gündra, "GIS-based planning and modeling for renewable energy: Challenges and future research avenues," *ISPRS IJGI*, vol. 3, no. 2, pp. 662–692, 2014.

[6] M. Brumenm, N. Lukac, and B. Zalik, "GIS application for solar potential estimation on buildings roofs," in *IARIA WEB*, 2015.

[7] B. Marion and M. Anderberg, "PVWATTS - an online performance calculator for grid-connected PV systems," in *ASES SOLAR*, 2000, pp. 119–124.

[8] PVGIS. http://re.jrc.ec.europa.eu/pvg_tools/en/tools.html.

[9] Mapdwell Solar System. http://www.mapdwell.com.

[10] L. de Sousa, C. Eykamp, U. Leopold, O. Baume, and C. Braun, "iguess-a web based system integrating urban energy planning and assessment modelling for multi-scale spatial decision making," in *iEMSs 2012*, 2012.

[11] S. Schuffert, "An automatic data driven approach to derive photovoltaic-suitable roof surfaces from ALS data," in *IEEE JURSE*, 2013, pp. 267–270.

[12] F. Kazhamiaka, Y. Ghiassi-Farrokhfal, S. Keshav, and C. Rosenberg, "Comparison of different approaches for solar PV and storage sizing," *IEEE TSUSC*, 2019.

[13] R. Atia and N. Yamada, "Sizing and analysis of renewable energy and battery systems in residential microgrids," *IEEE TSG*, vol. 7, no. 3, pp. 1204–1213, 2016.

[14] Y. Ghiassi-Farrokhfal, F. Kazhamiaka, C. Rosenberg, and S. Keshav, "Optimal design of solar PV farms with storage," *IEEE TSUSE*, vol. 6, no. 4, pp. 1586–1593, 2015.

[15] A. K. Shukla, K. Sudhakar, and P. Baredar, "Design, simulation and economic analysis of standalone roof top solar PV system in India," *Solar Energy*, vol. 136, pp. 437 – 449, 2016.

[16] M. Severini, A. Scorrano, S. Squartini, M. Fagiani, and F. Piazza, "SW framework for simulation and evaluation of partial shading effects in configurable PV systems," in *IEEE EEEIC*, 2016, pp. 1–6.

[17] P. Manganiello, M. Baka, H. Goverde, T. Borgers, J. Govaerts, A. van der Heide, E. Voroshazi, and F. Catthoor, "A bottom-up energy simulation framework to accurately compare PV module topologies under non-uniform and dynamic operating conditions," in *IEEE PVSC*, 2017, pp. 3343–3347.

[18] X. Gong and M. Kulkarni, "Design optimization of a large scale rooftop photovoltaic system," *Solar Energy*, vol. 78, no. 3, pp. 362 – 374, 2005.

[19] S. Kucuksari, A. M. Khaleghi, M. Hamidi, Y. Zhang, F. Szidarovszky, G. Bayraksan, and Y.-J. Son, "An integrated GIS, optimization and simulation framework for optimal PV size and location in campus area environments," *Applied Energy*, vol. 113, pp. 1601 – 1613, 2014.

[20] C. Keerthisinghe, G. Verbic, and A. C. Chapman, "Evaluation of a multi-stage stochastic optimisation framework for energy management of residential PV-storage systems," in *IEEE AUPEC*, 2014, pp. 1–6.

[21] W. Khemiri, R. Yaagoubi, and Y. Miky, "Optimal placement of solar photovoltaic farms using analytical hierarchical process and geographic information system in Mekkah, Saudi Arabia," in *Proc. of AIP*, 2018.

[22] S. Vinco, L. Bottaccioli, E. Patti, A. Acquaviva, E. Macii, and M. Poncino, "GIS-based optimal photovoltaic panel floorplanning for residential installations," in *Proc. of DATE*, 2018, pp. 437–442.

[23] L. Bottaccioli, E. Patti, E. Macii, and A. Acquaviva, "GIS-based software infrastructure to model pv generation in fine-grained spatio-temporal domain," *IEEE Systems Journal*, 2017.

[24] Weather Underground. http://www.wunderground.com.

[25] Mitsubishi Electric, "PV-MF165EB3 (165Wp)," https://www.mitsubishielectricsolar.com, 2004.

[26] D. J. Pagliari, S. Vinco, E. Macii, and M. Poncino, "Irradiance-driven partial reconfiguration of PV panels," in *Proc. of DATE*, 2019, pp. 884–889.

[27] S. Vinco, E. Macii, and M. Poncino, "Optimal topology-aware PV panel floorplanning with hybrid orientation," in *Proc. of ACM GLS-VLSI*, 2018, p. 491–494.

[28] Fixr, "Solar panel maintenance cost," https://www.fixr.com/costs/solar-panel-maintenance, 2020.